Antennas on Paper Using Ink-Jet Printing of Nano-Silver Particles for Wireless Sensor Networks in Train Environment

Dragos Dancila[1], Reza Moossavi[2], Johan Siden[2], Zhibin Zhang[1] and Anders Rydberg[1]

[1] Uppsala University, Angstrom Laboratory, Division of Solid-State Electronics, 751 21, Uppsala, Sweden

[2] Mid Sweden University, 851 70 Sundsvall, Sweden

e-mail: Dragos.Dancila@angstrom.uu.se

Abstract

This paper presents the design, manufacturing and measurements of antennas on paper, realized using ink-jet printing of conductive inks based on nano-silver particles (nSPs). The extraction of the substrate characteristics such as the dielectric constant and dielectric loss is performed using a printed ring resonator technique. The characterization of the nSPs conductive inks assesses different parameters as sintering time and temperature. Two antennas are realized corresponding to the most common needs for Wireless Sensor Networks (WSN) in Trains Environment. The first one is a patch antenna characterized by a broadside radiation pattern and suited for operation on metallic structures. The second one is a quasi-yagi antenna, with an end fire radiation pattern and higher directivity, without requiring a metallic ground plane. Both antennas present a good matching (S_{11} < -20 dB and S_{11} < -30 dB, respectively) and acceptable efficiency (55 % and 45 %, respectively) for the paper substrate used at the center frequency of 2.4 GHz, corresponding to the first channel of the IEEE 802.15.4 band.

1. Introduction

Transportation tags are increasingly used on trains, locomotives, chassis, containers, etc. with readers installed at strategic points, such as railroad interchange points, yards, gates, fuel tracks lanes, and maintenance facilities [1]. Tags encoded with unique IDs are linked wirelessly to the IT system providing information on the content, dimensions, customer and destination, providing an easy and inexpensive way to improve productivity and reduce costs. The IEEE 802.15.4 with bands around 2.45 GHz and 900 MHz are currently adopted and reliability and deployment tests are conducted towards the implementation of Wireless Sensor Networks in Train

Environment [2]. The multiplication of RFID tags and readers so far were mainly fabricated in PET substrates, but it is economically and environmentally more interesting to print the circuits directly on substrates made from cellulose [3]. In the same time, ink-jet printing of conductive materials is becoming an inexpensive alternative manufacturing method. Its easiness of use and low cost has turned it into a versatile printing method [4-5]. One of the various fields of application of conductive inks is antenna printing on various substrates, including paper, polymer films and textiles [6-7]. Paper printing is cheap and widely available, and is presently subject of various studies considering flexibility, humidity absorption, and substrate characteristics. One of current tags' drawbacks is the requirement of additional mechanical supports for placement at a 90-degree angle to the object, extending like a flag perpendicular to the object. With the tag not touching the object—particularly a metallic object—for improving readability [8]. On the other hand, cardboard boxes do not always provide the metallic ground plane required by some antennas, e.g. the patch antenna. Therefore, in addition of studying the manufacturing of nSPs conductive inks and paper substrates, we investigate two different antenna designs, suited for each of the two mentioned implementations, i.e. with and without metallic ground plane best suited for Wireless Sensor Networks in Train Environment. The first antenna investigated is a patch antenna characterized by a broadside radiation pattern and suited for operation on metallic structures. The second one is a quasi-yagi antenna, with an end fire radiation pattern and higher directivity, without requiring a metallic ground plane.

2. Manufacturing

The study is devised in measuring inks conductivity (σ) and is using a printed ring resonator for measuring dielectric characteristics as electrical conductivity (ϵ_r) and dielectric loss tangent ($\tan\delta$). These parameters are required for the antenna design and feeding microstrip lines [9].

a. Characterization of conductive inks

Nano Silver-Particles inks (NSP-JL series silver ink paste), manufactured by Harima Chemicals Group, Japan [10] have been used to shape antennas on paper. The ink consists of silver nano-particles with an average particle size of 7 nm. The sintering temperature recommended by the manufacturer is between 120°C and 150°C. For measuring the conductivity, a 1.5µm tick pattern is printed on a 240 µm thick

photo paper substrate [11], see Figure 1. The printing of 1.5µm tick traces is performed using a Dimatix Materials Printer DMP-2800 [12]. Once the samples dried at room temperature, their conductivity is measured by means of a 4 probe parametric analyzer. Later, each sample is sintered by heating in a furnace at different temperatures (80°C ~ 180°C, in steps of 10°C) and conductivity is measured a second time, see Figure 2. The electrical conductivity (σ) of the silver ink is compared to the electrical conductivity of bulk materials such as silver ($\sigma = 6.30 \times 10^7$ S/m), copper ($\sigma = 5.96 \times 10^7$ S/m), gold ($\sigma = 4.10 \times 10^7$ S/m) and aluminum ($\sigma = 3.50 \times 10^7$ S/m), see Figure 2. The impact of the sintering time on conductivity is also investigated. For this purpose, samples have been heated at fixed temperatures (120°C, 150°C and 180°C). Electrical conductivity has been measured after 15, 30, 45, 60, 90 and 120 minutes, as can be seen Figure 3. After 60 minutes heating at 180°C, a minor change in the color of the paper is observed. The conductivity does not change after sintering for 90 minutes and only a marginal difference between sintering at 150°C and 180°C is measurable, as can be deduced from Figure 3. Therefore, it is concluded that the best sintering temperature is 150°C with the temperature maintained during 90 minutes.

b. Extraction of the dielectric characteristics of the paper substrate

One of the important factors in designing planar antennas is the dielectric characterization of the substrate, particularly the relative permittivity (ϵ_r) and dielectric losses (tan δ) in the substrate. Permittivity is frequency dependent [13] and for studying such characteristics a technique based on a ring resonator is implemented [14]. The ring resonator, used for dielectric characterization is shown in Figure 4. The ring is made with printed traces and a thick copper is used as ground. The ring presents resonances for the mean circumference equal to the integral values of the guided wavelength (λ_g) [15]. For a microstrip ring, λ_g is calculated as:

$$2\pi r = n\lambda_g, for n = 1,2,3,\ldots \quad (1)$$

$$\lambda_g = \frac{\lambda}{\sqrt{\epsilon_{eff}}} = \frac{1}{\sqrt{\epsilon_{eff}}}\frac{c}{f} \quad (2)$$

Replacing λ_g with its equivalent value from (1) and (2) resulting in:

$$f_n = \frac{nc}{2\pi r\sqrt{\epsilon_{eff}}}, \quad \text{for } n = 1,2,3,\ldots \quad (3)$$

The relationship between the resonance frequency and the effective relative dielectric constant (ϵ_{eff}) is given by (3). Using (3), a ring resonator is designed to resonate at 2.4 GHz. Table 1 shows the calculated values for the ring. Using a vector network analyzer the effective dielectric constant is measured. Meanwhile, a simulation is made based on the dimensions in Table 1 to confirm the validity of the results obtained (Figure 5).

$\tan(\delta)$ is calculated using (4) [9,16]:

$$\tan(\delta) = \frac{\alpha_d \lambda_0 \sqrt{\epsilon_{eff}}(\epsilon_r - 1)}{\pi \epsilon_r (\epsilon_{eff})} \tag{4}$$

where λ_0 is free-space wavelength, $\alpha_d$is the attenuation due to substrate, ϵ_r and $\epsilon_{eff}$are dielectric constant and effective dielectric constant respectively. Figure 5 shows the measurement results in comparison with the simulation results. Measuring the ring resonator, with the help of (3) and (4), both the substrate's dielectric constant and loss tangent are calculated, as can be seen in Table 2. This extracted information is of great importance in the following antenna design, since they affect the dimensions of antenna and feeding lines and allow to characterize further the performance of the antennas, as we will see in the next part.

3. Antenna Design

a. Patch Antenna

A patch antenna is implemented as an nSP printed patch trace, feeded by a microstrip line and mounted on a tick copper plate, the ground plane. The dimensions of the patch antenna are calculated by using standard patch antenna equations as (5) – (8) from [9].

$$W = \frac{1}{2\mathrm{f}\sqrt{\mu_0 \epsilon_0}} \sqrt{\frac{2}{\epsilon_r + 1}} = \frac{c}{2\mathrm{f}} \sqrt{\frac{2}{\epsilon_r + 1}} \tag{5}$$

$$\epsilon_{eff} = \frac{\epsilon_r + 1}{2} + \frac{\epsilon_r - 1}{2} [1 + 12 \frac{h}{W}]^{-1/2}, W/h > 1 \tag{6}$$

$$\frac{\Delta L}{h} = 0.412 \frac{(\epsilon_{eff} + 0.3)(\frac{W}{h} + 0.264)}{(\epsilon_{eff} - 0.258)(\frac{W}{h} + 0.8)} \tag{7}$$

$$L = \frac{\lambda_g}{2} - 2\Delta L \quad (8)$$

The dimensions of the designed antenna are as follows: patch width = 50.8 mm, length = 43.8 mm, inset = 13.23 mm and feed width = 78 µm, length = 30 mm. The height of the paper substrate is 240 µm and the permittivity used is 2.029 and tan δ = 0.079.

b. Quasi–Yagi Antenna

Quasi–Yagi antenna consists of 2 parts a driver and a director [17]. The driver is a dipole antenna with 2 symmetrical parts, each equal to a quarter of the guided wavelength ($\lambda_g/4$), comprising ungrounded metal rods or strips and is fed by two balanced feeding lines. Feeding dipoles through coaxial cables (which are unbalanced feeding lines) requires an adapter to convert such an unbalanced line into a balanced feed [9]. The balun creates a 180° degrees phase difference at the center of the dipole. There are different techniques for designing a balun from which, the Microstrip-to-Coplanar stripline (CPS), introduced by Qian and Itoh [18], is used in this experiment. Figure 11 shows the balun used to feed the CPS. This balun is connected to 75Ω quarter-wavelength CPS to feed the dipole. All dimensions of the design (dipole and balun) are reported in Table 3. The height of the paper substrate is 240 µm and the permittivity used is 2.029 and tan δ = 0.079.

4. Measurements results

a. Patch Antenna

Measurements of the patch antenna printed on paper above the ground coper plate are compared to the simulations realized with HFSS using the dielectric characteristics of the paper extracted in Section I. An overall good agreement between simulations and measurements is observed. The measurement of the return loss (S11) is shown in Figure 7 and in the Smith chart in Figure 8. A slight phase discrepancy occurs between measurements and simulations which may be due to the SMA connector which is not simulated. The far-field radiation measurement of this antenna is conducted in an anechoic chamber, using a stationary Vivaldi antenna as the receiver and the designed patch as the rotating transmitter. The measurements are performed in E and H fields with both co- and cross-polarization. Figure 9 shows the radiation pattern in the E and Figure 10, in the H

plane with, as expected a maximum on the broadside for the co-polarization. The efficiency of the antenna is measured in a reverberation chamber [19]. The total efficiency of the antenna is -2.59 dB or 55%.

b. Quasi–Yagi Antenna

While Figure 11 shows the design dimensions related to Table 3, Figure 12 shows the entire construction of the antenna. The transmission lines are using a copper plate attached on the back side of the paper substrate as ground plane reference. The ground plane does not continue underneath the 75Ω CPS feeds since these are in balanced configuration. To ensure the transition from an unbalanced to a balanced configuration a balun is implemented. As can be seen Figure 13, the return loss (S11) of the full structure antenna with balun presents some losses (-5dB) outside the antenna's resonance. These are due to the high tan δ and relatively long transmission lines (λ/4) of the balun. As a result, the resonance's locus is closer to the center of the Smith chart, in Figure 14. The radiation patterns measurements are performed in E and H fields with both co- and cross-polarization. Figure 15 shows the radiation pattern in the E and Figure 16, in the H plane. The maximum in the E plane is slightly tilted downwards pointing towards a maximum at 150°. The total efficiency of the antenna is -3.46 dB or 45%.

5. Discussions and Conclusions

The manufacturing and performance of the antennas on paper, realized using ink-jet printing of conductive inks is dependent on several manufacturing parameters, such as sintering time, with an optimal of 90 minutes and temperature with an optimal of $150°C$. Dielectric characteristics of the substrate, permittivity ($\epsilon_r = 2.029$) and dielectric losses (tan δ =0.084) have been extracted using a ring resonator for the paper substrate of 250 μm thickness. These parameters have been used in HFSS simulation for designing two antennas, a broad side patch antenna and an end fire radiation quasi-yagi antenna, with resulting efficiency 55% and 45% respectively. The antennas are quite narrow band around a central frequency of 2.4 GHz and correspond to the most common needs for Wireless Sensor Networks (WSN) on Trains.

REFERENCES

[1] http://www.transcore.com/. Rail Applications projects. Access 14-04-15.
[2] M.Grudén, A.Westman, J.Platbardis, P.Hallbjörner, A.Rydberg, “Reliability Experiments for Wireless Sensor Networks in Train Environment”, Wireless Technology Conference 2009. EuWIT 2009, European, Rome.
[3] F. Eder, H. Klauk, M. Halik, Dehm,“ Organic electronics on 14, pp.2673-2675, 5 April 2
[4] V. Kantola, J. Kulovesi, L. Lahti, R. Lin, M. Zavodchikova, and E. Coatanéa, “Printed Electronics, Now and Future,” in in Bit Bang Rays to the Future, Helsinky: Helsinki University Print, 2009, pp. 63–102.
[5] J. Krumm et al., “Printed Electronics - First Circuits, Products and Roadmap,” in in Analog Circuit Design, H. Casier, M. Steyaert, and A. H. M. van Roermund, Eds. Dordrecht: Springer Netherlands, 2011, pp. 333–345.
[6] A. Rida, “Conductiver Inkjet Printed Antennas on Flexible Low-Cost Paper-Based Substrates for RFID and WSN Applications,” Georgia Institute of Technology, 2009.
[7] J. Sidén, M. K. Fein, A. Koptyug, and H.-E. Nilsson, “Printed antennas with variable conductive ink layer thickness,” IET Microwaves, Antennas Propag., vol. 1, no. 2, p. 401, 2007.
[8] http://www.rfidjournal.com/articles/view?3306 “ThyssenKrupp to Use EPC UHF Tags to Track Steel”. Access. 14-04-15.
[9] C. A. Balanais, Antenna Theory: Analysis and Design, 3rd. ed. Wiley-Interscience, 2005.
[10] Harima Chemical Group - http://www.harima.co.jp/en
[11] Anker International PLC - photo paper GLOSS finish 6×4".
[12] http://www.fujifilmusa.com/products/industrial_inkjet_printheads/deposition-products/dmp-2800/index.html
[13] A. R. Von Hippel, Dielectrics and Waves, no. v. 1. Artech House, Incorporated, 1954.
[14] A. Rida et al., “Novel Manufacturing Processes for Ultra-Low-Cost Paper-Based RFID Tags with Enhanced ‘Wireless Intelligence’,” 2007 Proc. 57th Electron. Components Technol. Conf., pp. 773–776, 2007.
[15] O. Vasylchenko, “Towards the miniaturization of new ultra wideband,” Katholieke Universiteit Leuven, 2010.
[16] K. Chang, Microwave Ring Circuits and Antennas. John Wiley & Sons., 1996.
[17] N. Kaneda, W. R. Deal, Y. Qian, R. Waterhouse, and T. Itoh, “A broadband planar quasi-Yagi antenna,” Antennas Propagation, IEEE Trans., vol. 50, no. 8, pp. 1158–1160, 2002.
[18] Y. Qian and T. Itoh, “A broadband uniplanar microstrip-to-CPS transition,” in Microwave Conference Proceedings, 1997. APMC ’97, 1997 Asia-Pacific, 1997, pp. 609–612 vol.2.
[19] Grudén, M. (2014). Wireless Sensor Network Systems in Harsh Environments and Antenna Measurement Techniques. (Doctoral dissertation). Uppsala: Acta Universitatis Upsaliensis.

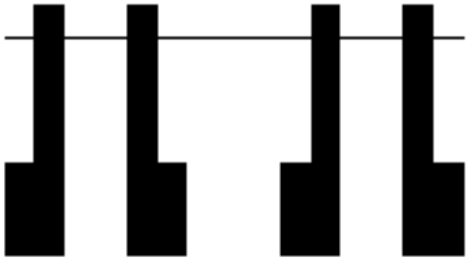

Figure 1: Test pattern for measuring the conductivity of the nano-silver particles (nSP) ink.

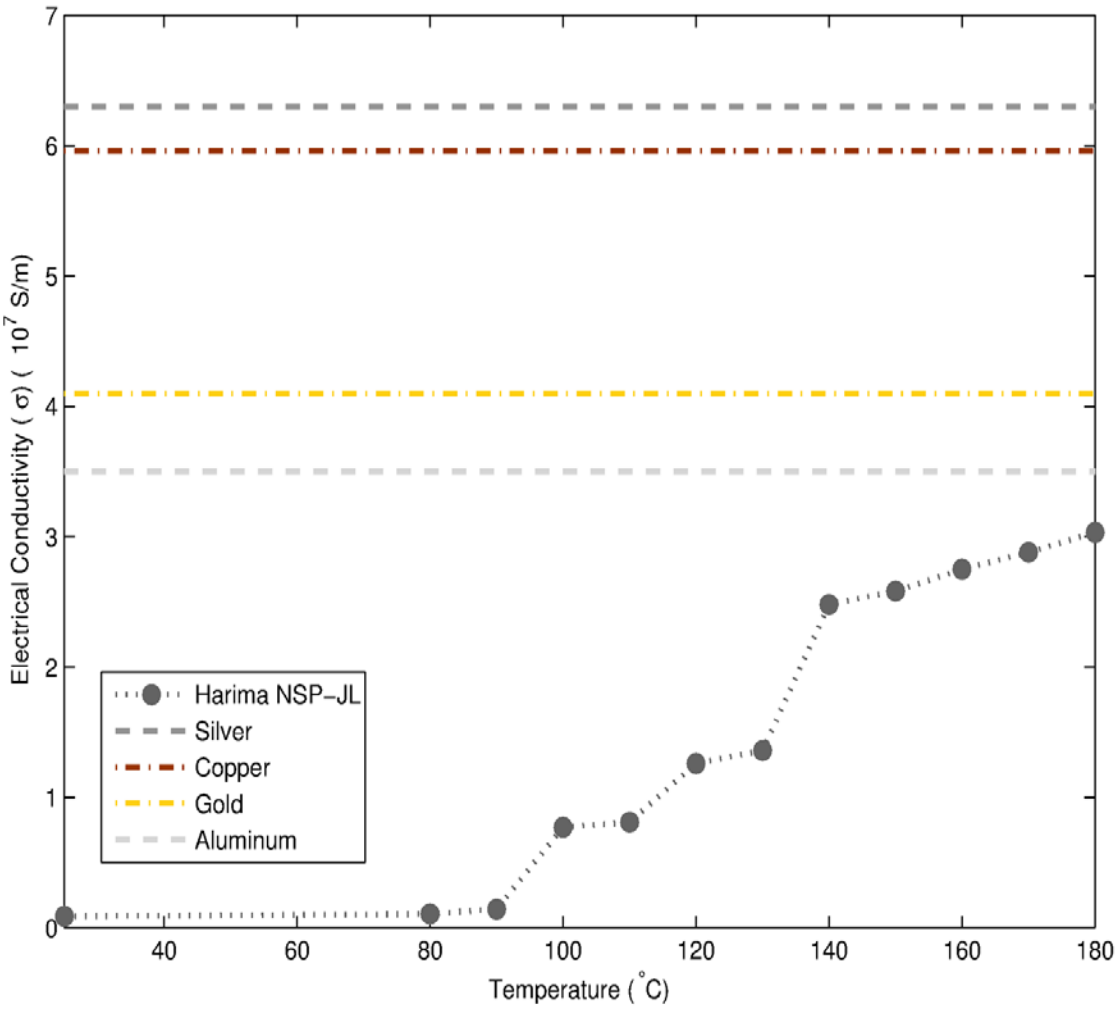

Figure 2: Electrical conductivity of Harima NSP-JL ink as result of sintering temperature.

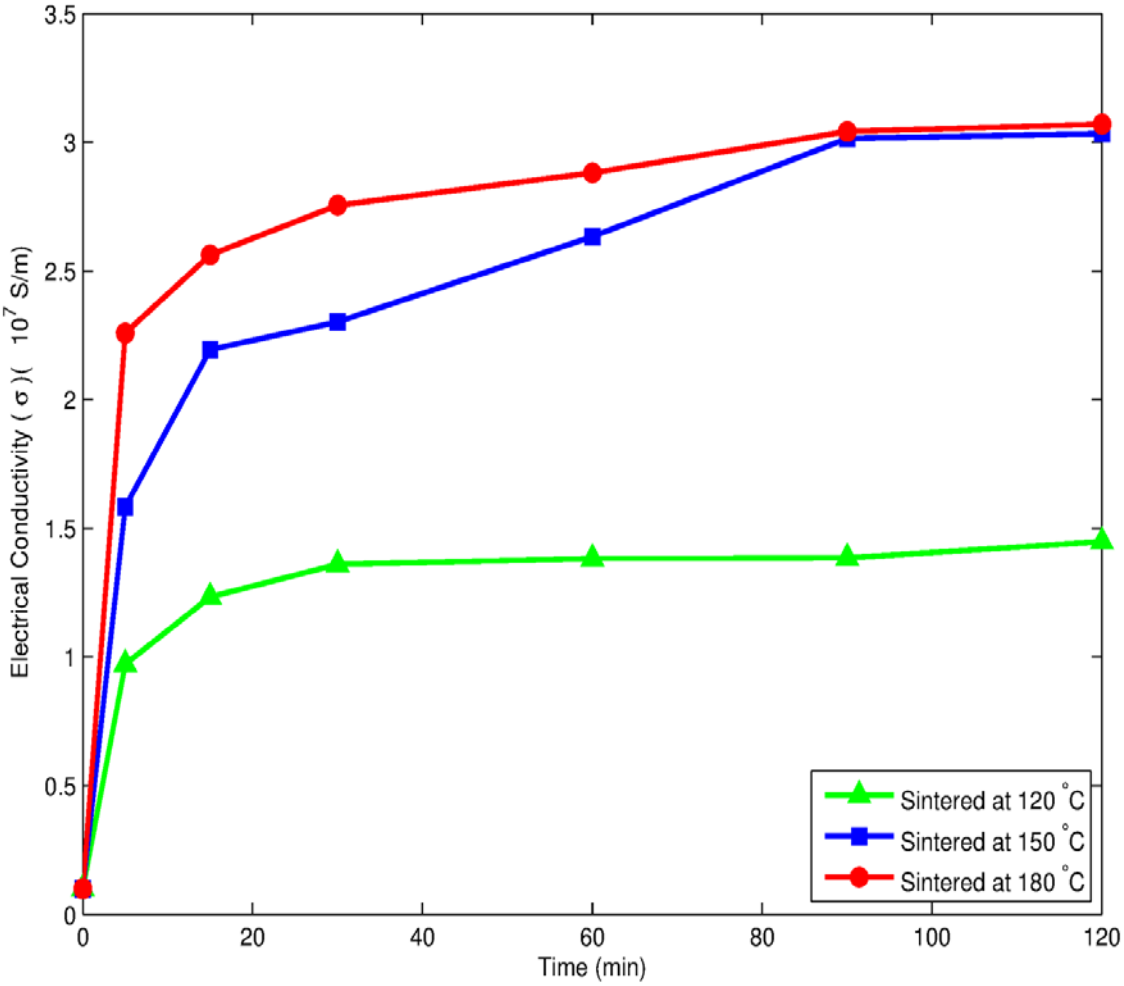

Figure 3: Electrical conductivity of Harima NSP-JL ink as result of sintering time.

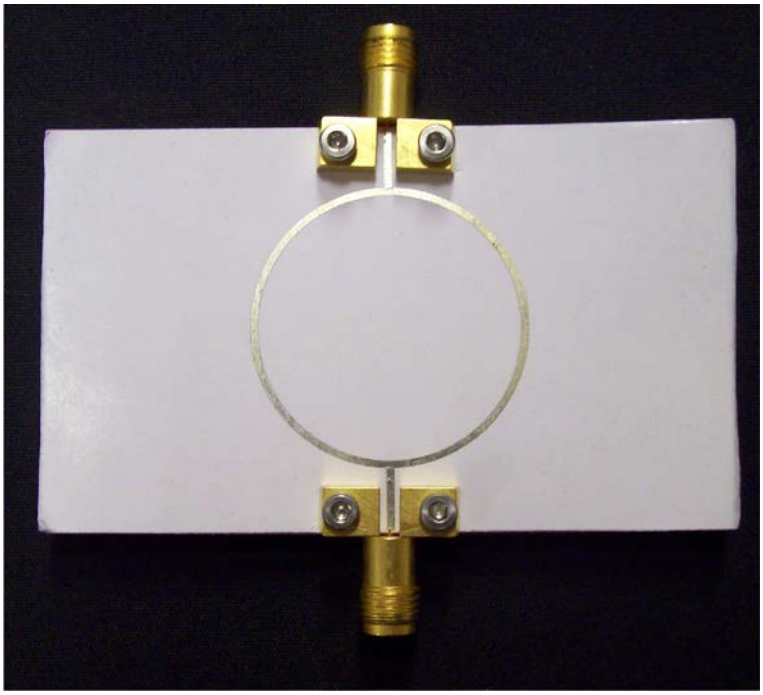

Figure 4: Printed ring resonator on paper substrate.

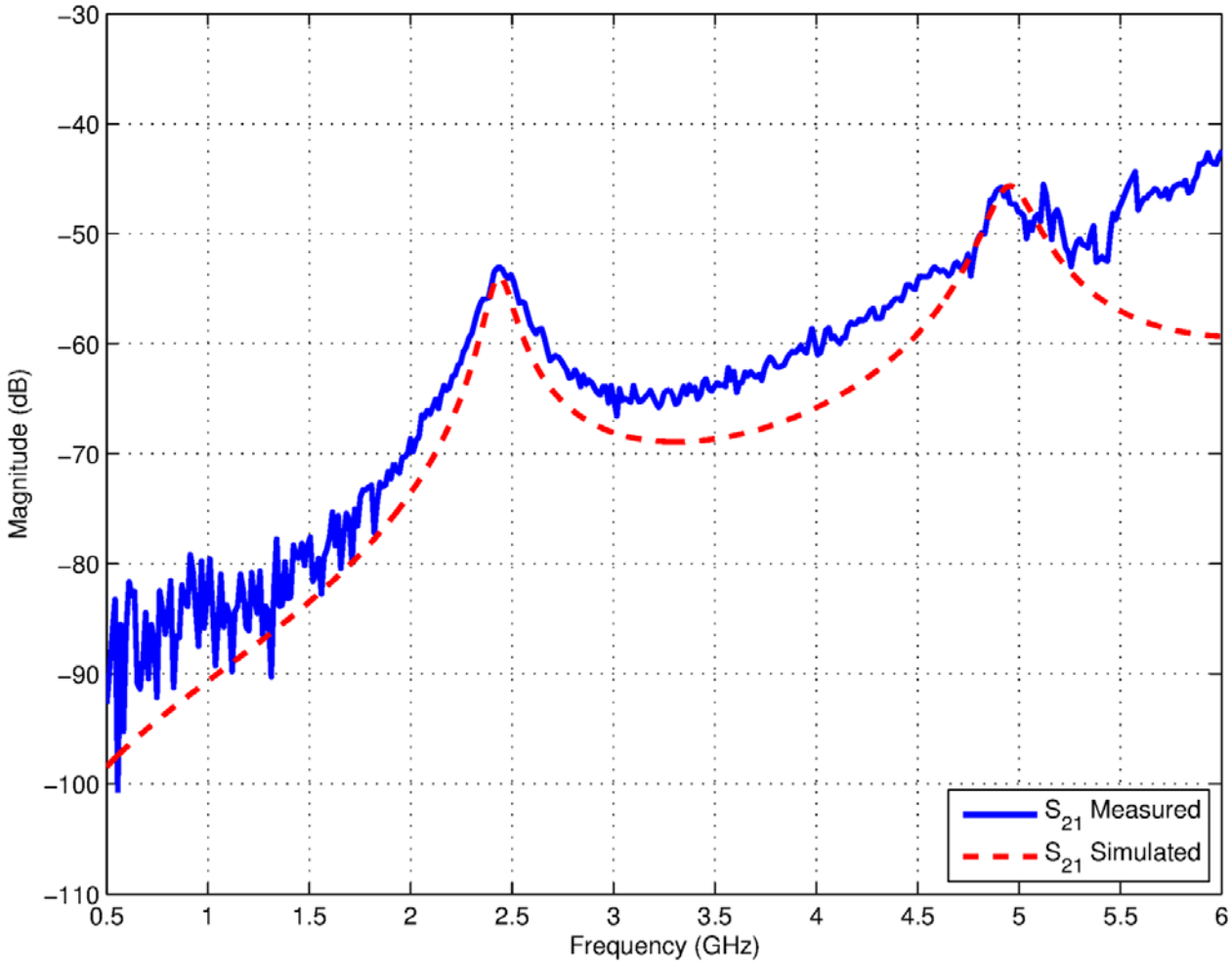

Figure 5: S21 magnitude for ring resonator.

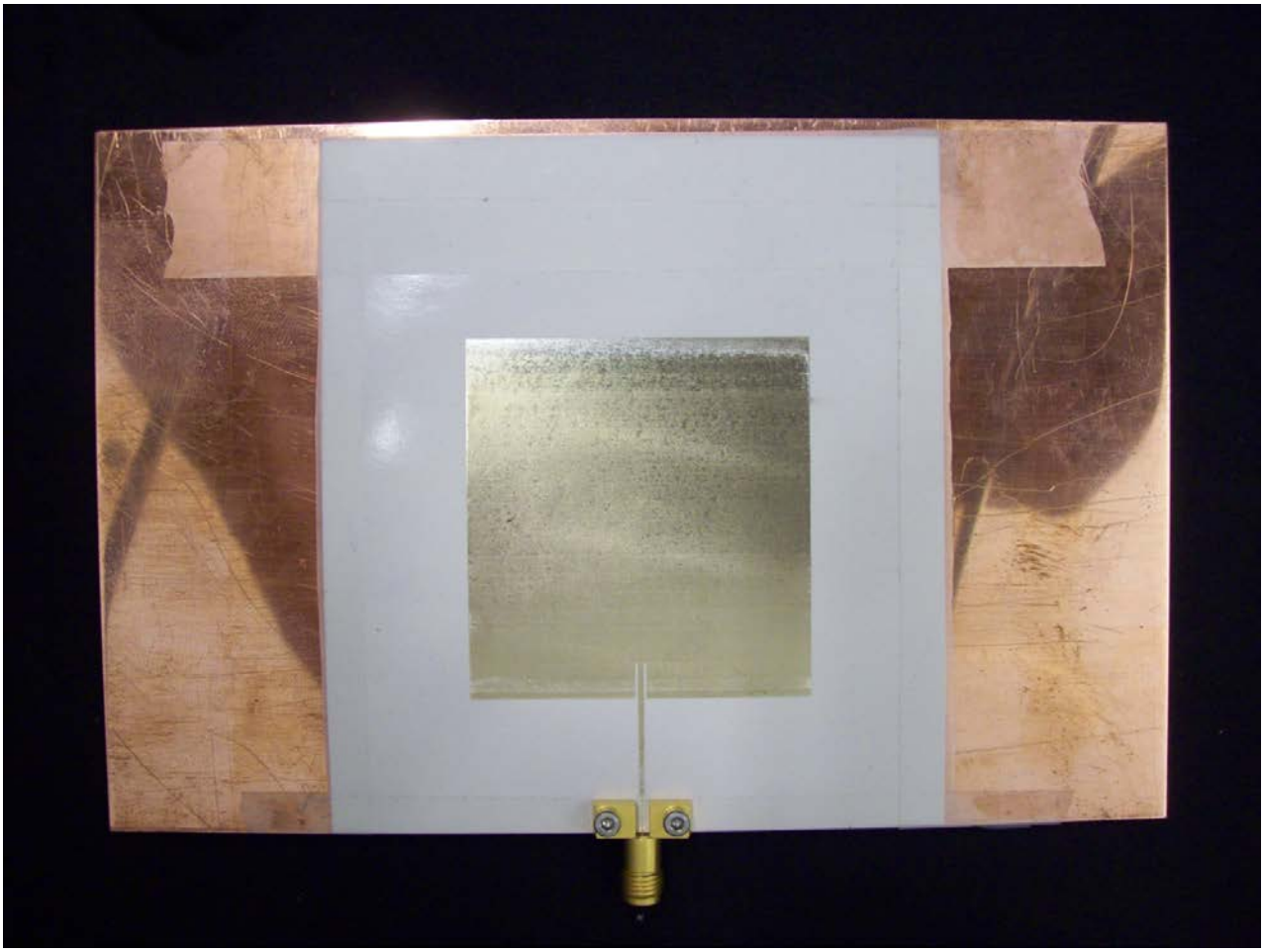

Figure 6: Microstrip patch antenna.

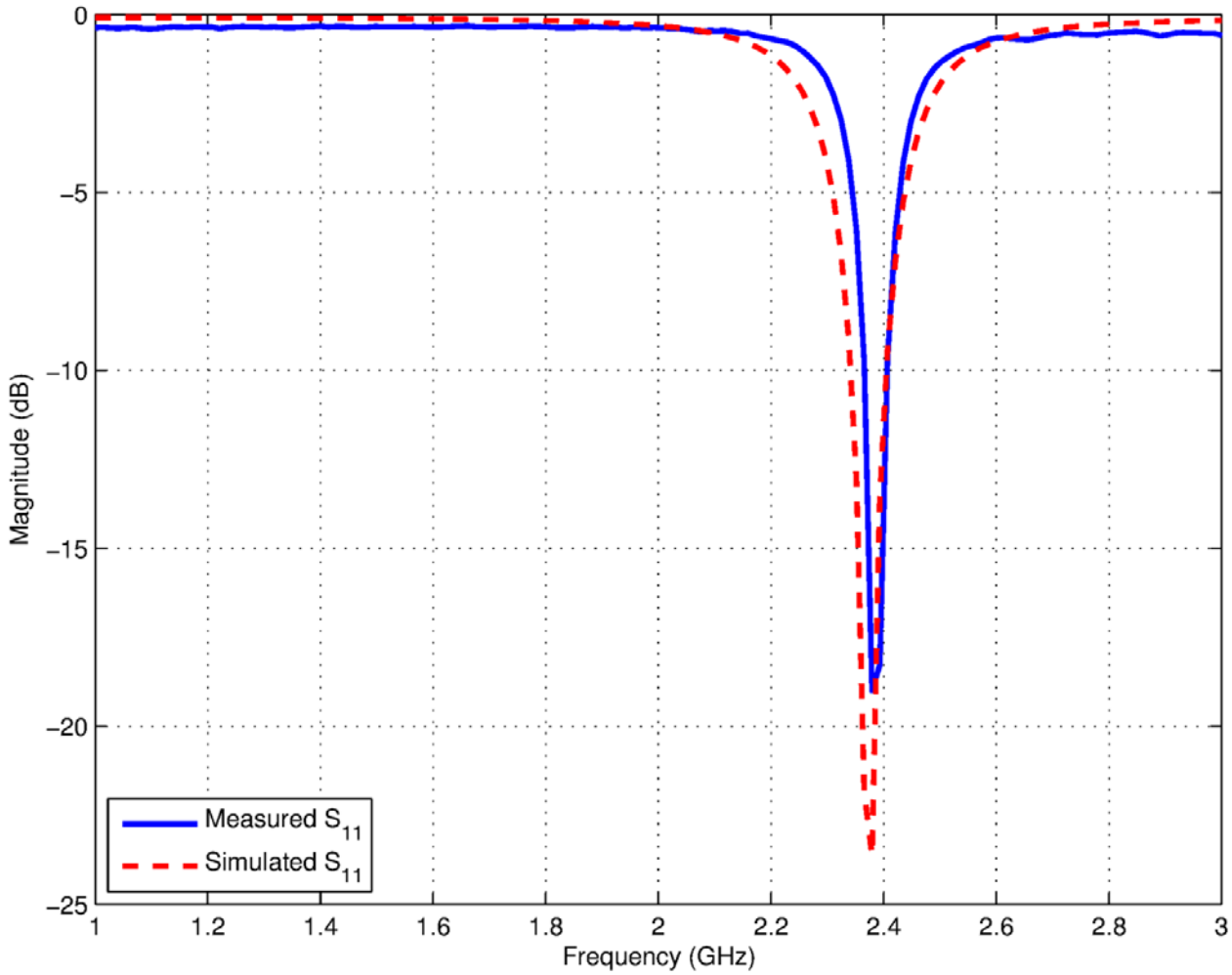

Figure 7: S11 magnitude for simulated and actual patch antenna.

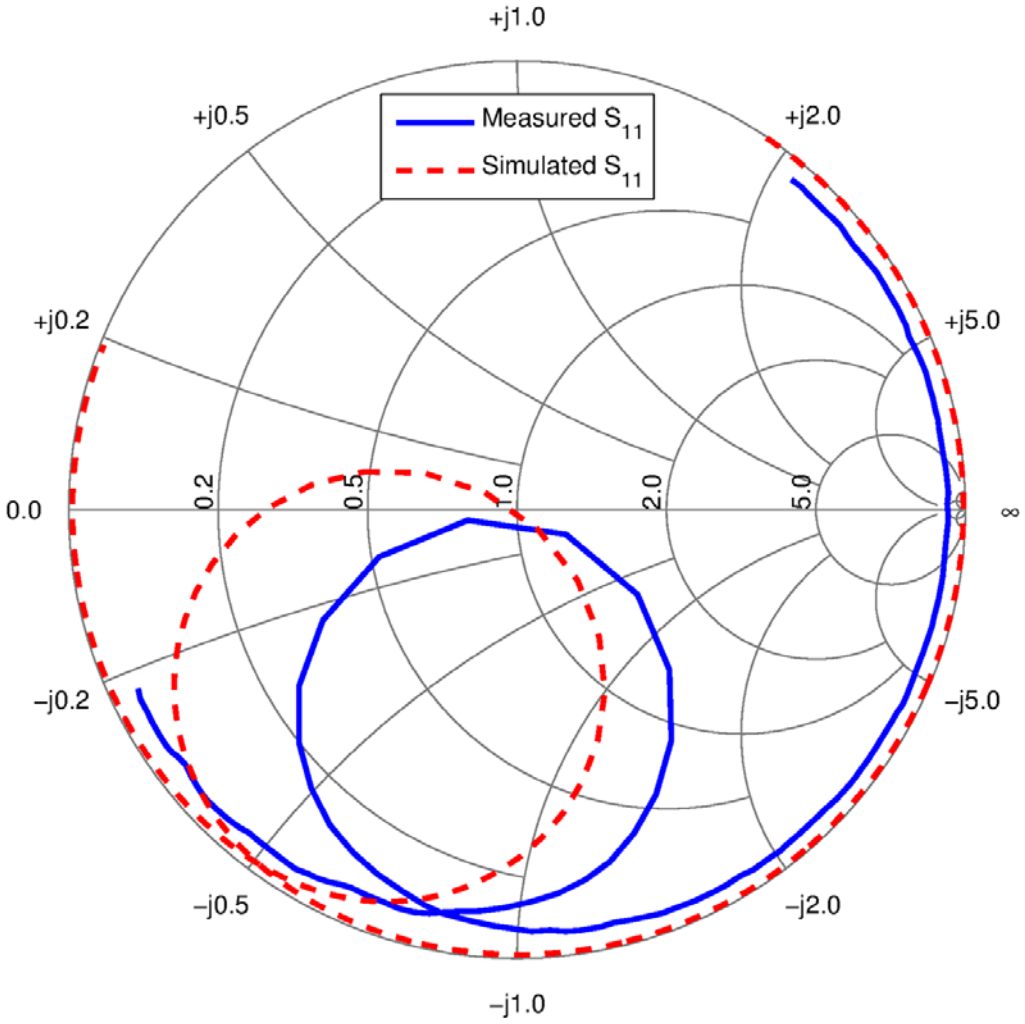

Figure 8: Smith chart for actual and simulated patch antenna.

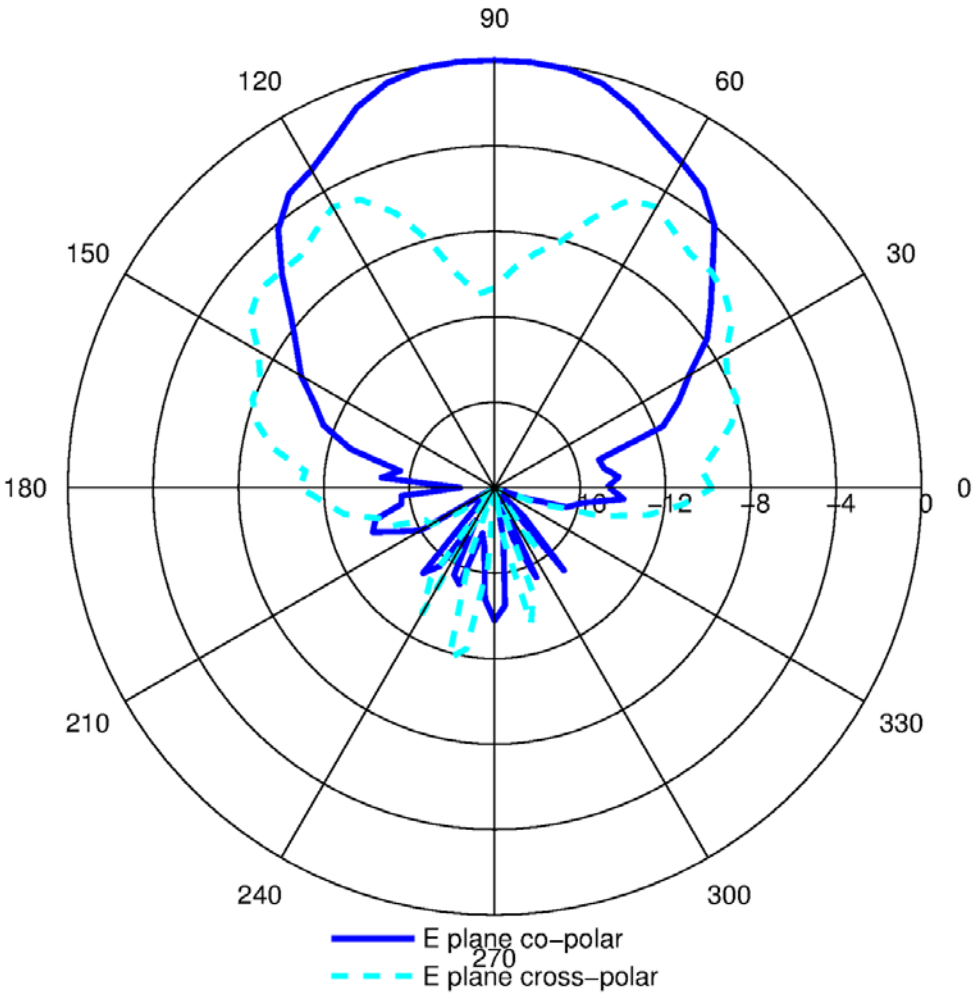

Figure 9: Radiation pattern for patch antenna (E-plane).

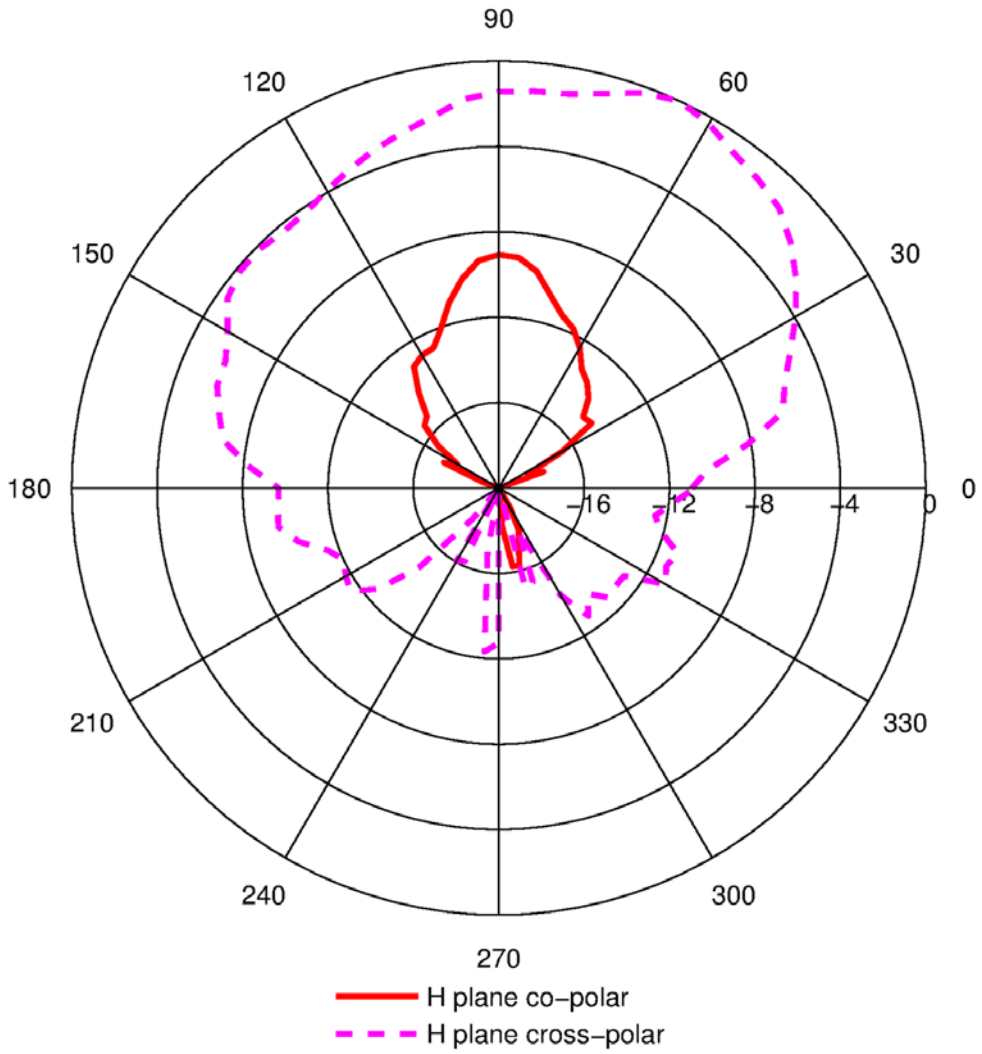

Figure 10: Radiation pattern for patch antenna (H-plane).

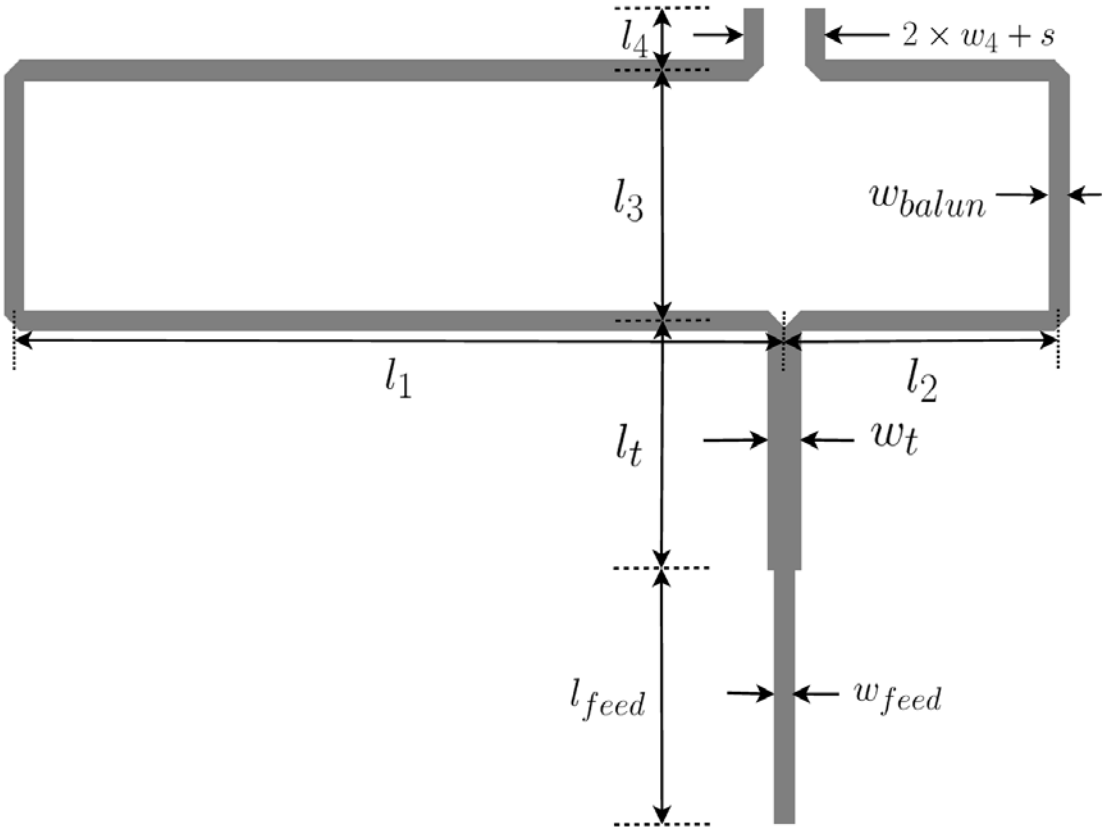

Figure 11: 2.4GHz Balun for Quasi-Yagi antenna feed.

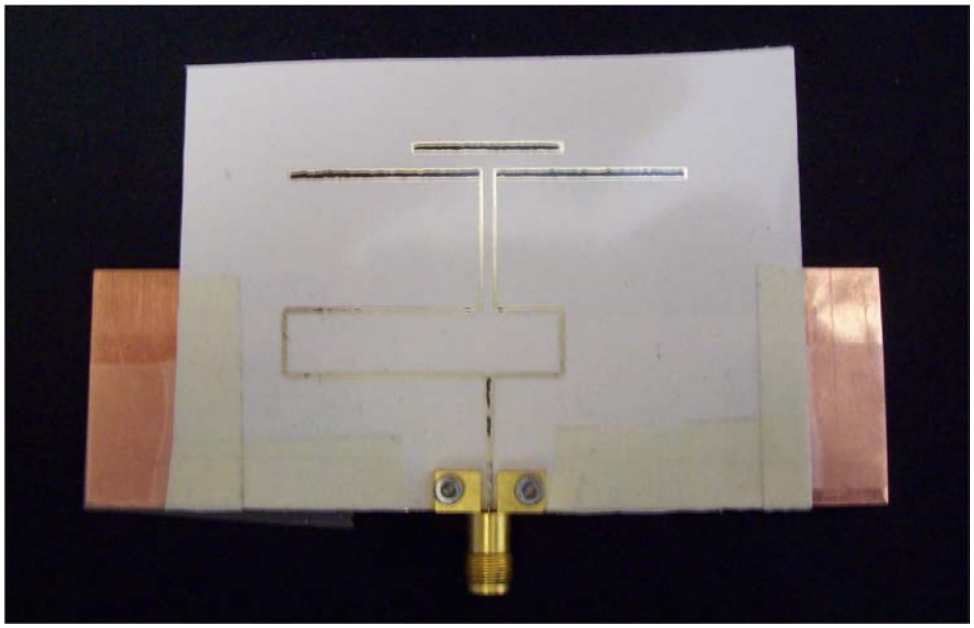

Figure 12: Quasi-Yagi antenna printed on paper.

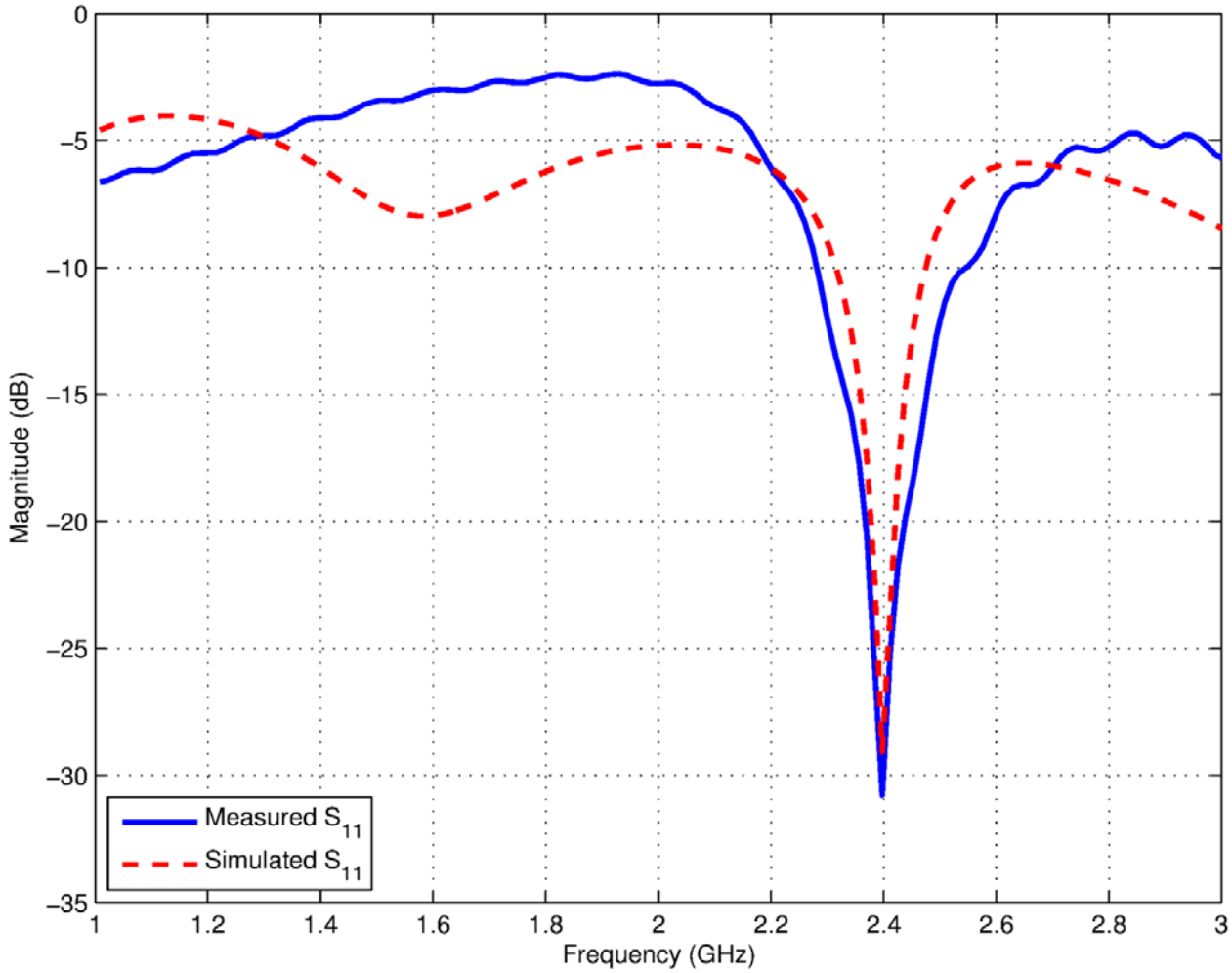

Figure 13: S11 magnitude plot for simulated and actual Quasi-Yagi antenna.

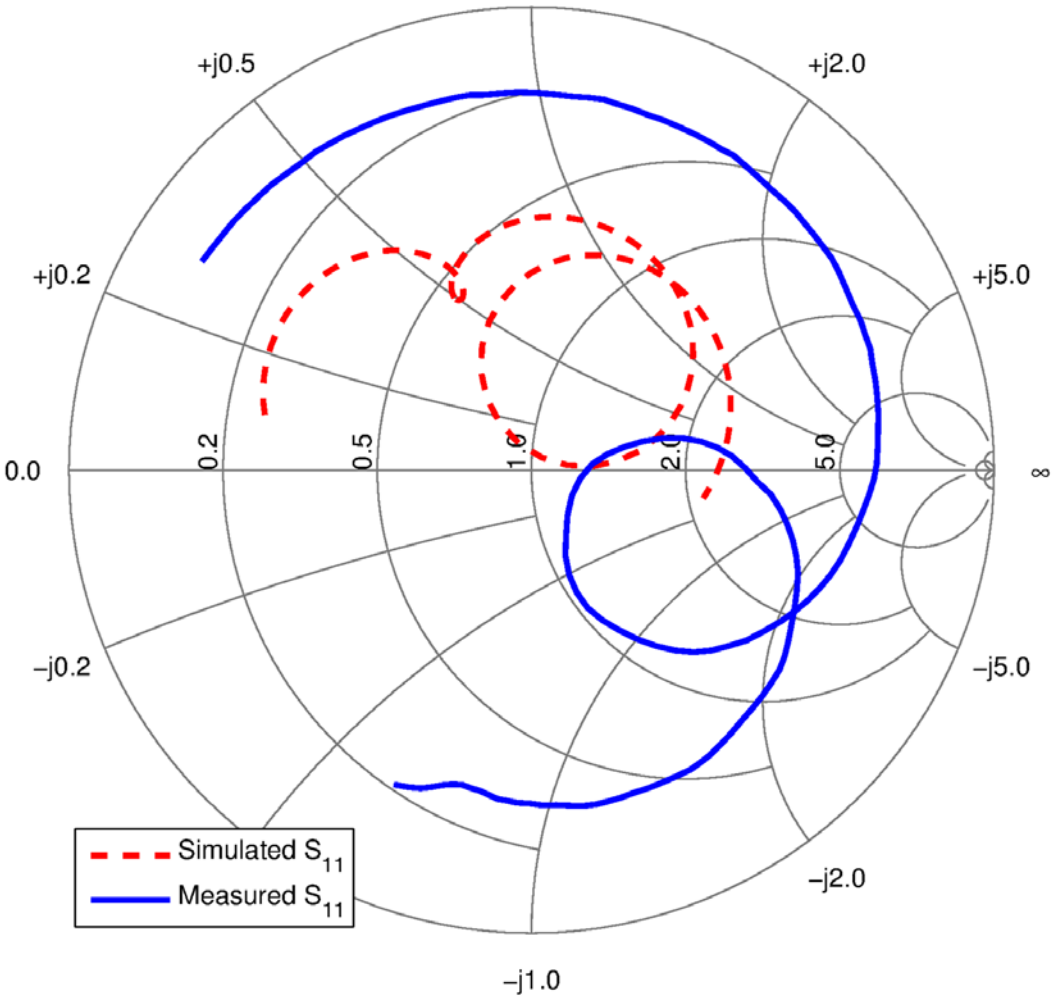

Figure 14: Smith chart for actual and simulated Quasi-Yagi antenna.

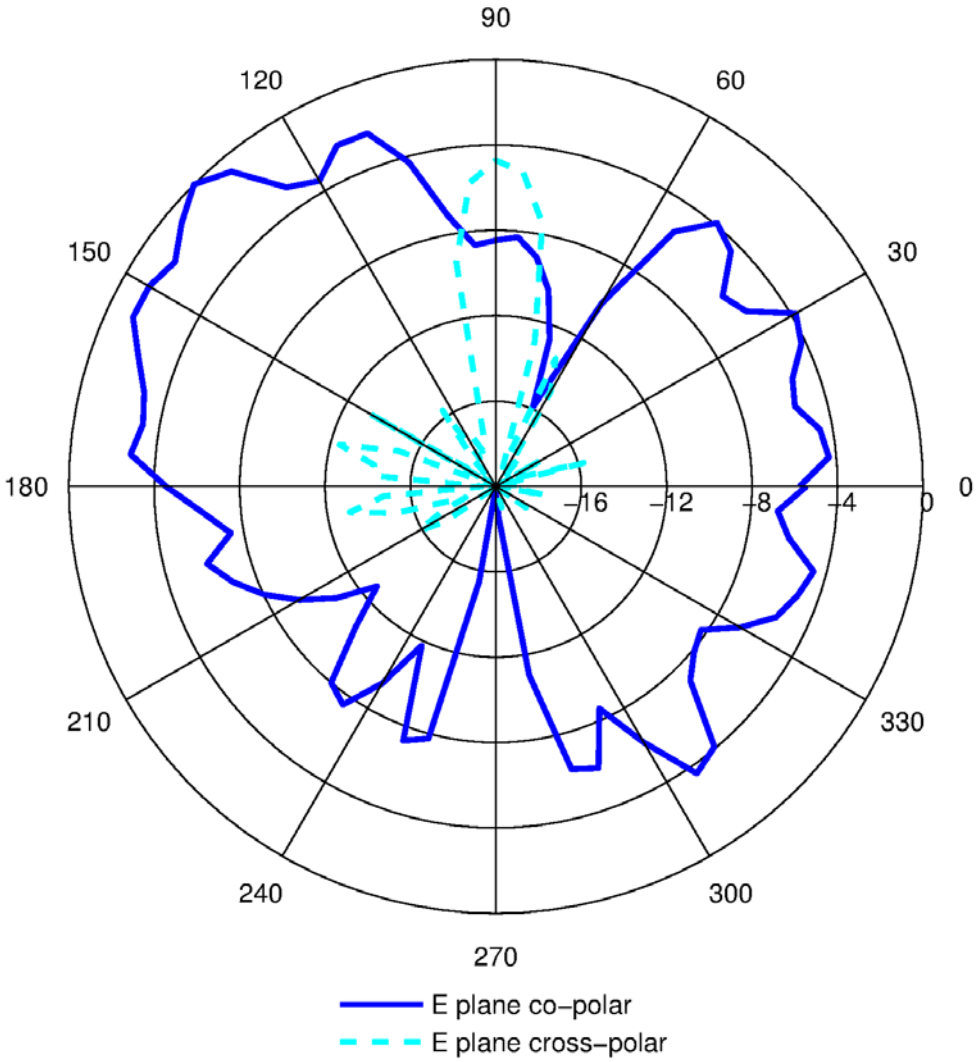

Figure 15: Radiation pattern for Quasi-Yagi antenna (E-plane).

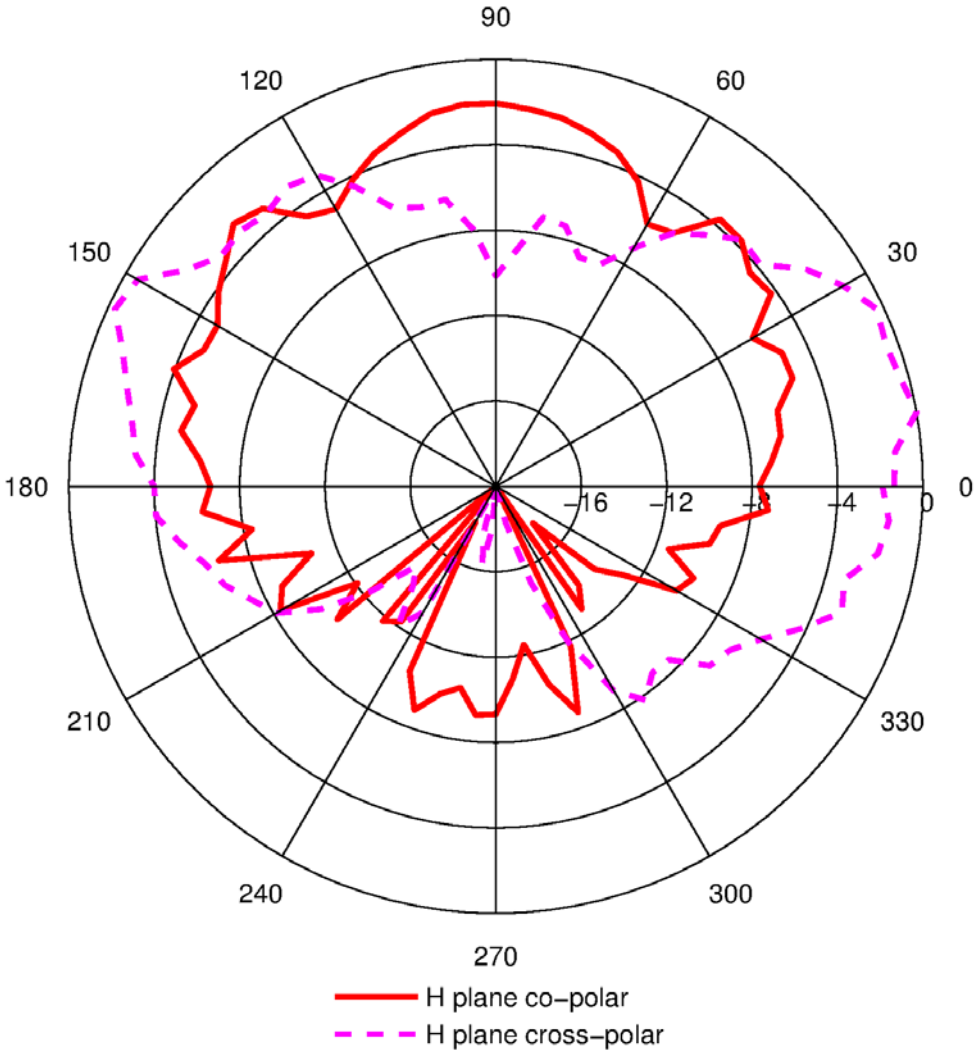

Figure 16: Radiation pattern for Quasi-Yagi antenna (H-plane).

Ring resonator dimensions	
Feed line length	5 mm
Feed line width	500 µm
Ring line width	500 µm
Coupling gap	100 µm
Ring mean radius	13.75 mm

Table 1: Ring resonator dimensions.

	Resonant frequency (f) (GHz)	Insertion loss ($\|S_{21}\|$) (dB)	BW-3dB (MHz)	ϵ_r	$\tan(\delta)$ Calculated	Measured
n = 1	$f_1 = 2.439$	-51.03	206	2.029	0.079	0.084
n = 2	$f_2 = 4.914$	-45.8	179	1.997	0.033	0.036

Table 2: Extracted dielectric characteristics for paper substrate

Symbol	Description	Size
w_{feed}	Width of feeding line	0.78 mm
w_t	Width of T-junction	1.26 mm
w_{balun}	Width of balun lines	0.78 mm
w_4	Width of balun output	0.78 mm
w_{bf}	Width of balanced feed	0.42 mm
w_{dip}	Width of dipole antenna	1.4 mm
l_{feed}	Length of feeding line	8.83 mm
l_t	Length of T-junction	8.71 mm
l_1	Length of balun's long arm	27.46 mm
l_2	Length of balun's short arm	9.81 mm
l_3	Length of balun extension	8.71 mm
l_4	Length of balun output	2.21 mm
l_{bf}	Length of balanced feed	16.96 mm
l_{dip}	Length of dipole antenna	54.49 mm
s	Dipole gap	1.4 mm

Table 3: Quasi-Yagi and balun dimensions.